Wind and Structures, Vol. 15, No. 6 (2012) 495-508
DOI: http://dx.doi.org/10.12989/was.2012.15.6.495

Acrosswind aeroelastic response of square tall buildings: a semi-analytical approach based of wind tunnel tests on rigid models

I. Venanzi* and A.L. Materazzi

Department of Civil and Environmental Engineering, University of Perugia, Perugia, Italy
(Received March 24, 2011, Revised May 23, 2012, Accepted June 19, 2012)

Abstract. The present paper is focused on the prediction of the acrosswind aeroelastic response of square tall buildings. In particular, a semi-analytical procedure is proposed based on the assumption that square tall buildings, for reduced velocities corresponding to operational conditions, do not experience vortex shedding resonance or galloping and fall in the range of positive aerodynamic damping. Under these conditions, aeroelastic wind tunnel tests can be unnecessary and the response can be correctly evaluated using wind tunnel tests on rigid models and analytical modeling of the aerodynamic damping. The proposed procedure consists of two phases. First, simultaneous measurements of the pressure time histories are carried out in the wind tunnel on rigid models, in order to obtain the aerodynamic forces. Then, aeroelastic forces are analytically evaluated and the structural response is computed through direct integration of the equations of motion considering the contribution of both the aerodynamic and aeroelastic forces. The procedure, which gives a conservative estimate of the aeroelastic response, has the advantage that aeroelastic tests are avoided, at least in the preliminary design phase.

Keywords: aeroelastic force; aerodynamic damping; tall buildings; wind tunnel tests; rigid models; square cross-section

1. Introduction

The prediction of the wind response of tall buildings requires special attention during the design stage. While the alongwind aerodynamic damping is always positive and almost linearly increases with the reduced velocity, the acrosswind aerodynamic damping often shows a monotonic growth for low reduced velocities. However, it can become negative beyond a certain reduced velocity which depends on many factors, e.g., the structural shape, the wind speed, the building's natural frequency, the turbulence intensity and the structural damping ratio (Marukawa *et al*. 1996, Wu *et al*. 2010). Negative aerodynamic damping in flexible structures is associated with the occurrence of vortex excited oscillation and galloping (Kawai 1992, 1998). The vortex shedding resonance can theoretically occur at a reduced frequency corresponding to the Strouhal number (Vickery and Steckley 1993, Amandolese and Hemon 2010). Alternatively, the response can be governed by galloping, an instability phenomenon typical of non circular slender structures, due to null or negative damping (Novak 1972).

* Corresponding author, Dr., E-mail: ilaria.venanzi@strutture.unipg.it

In the recent years also the interesting case of buildings whose section varies with the height through taper and set-back began to be addressed (Kim and Kanda 2010).

The first references on the acrosswind aeroelastic response of flexible structures are dated back to the early '70s, when many authors discussed the basic aeroelastic instability problem for square and rectangular tall buildings. In Novak (1972), an analytical model of the galloping instability is proposed. In Washizu *et al.* (1978), an experiment-based method for the evaluation of galloping and vortex induced response is developed. In Kwok and Melbourne (1981), experimental results of aeroelastic tests are presented and a prediction procedure based on a random excitation model is proposed.

In 1992 Boggs pointed out that ignoring aeroelastic effects leads in general to slightly conservative results except under certain conditions, e.g., vortex shedding or galloping. In his paper, an aeroelastic magnification ratio (AMF), that represents the amplification of the aeroelastic acrosswind response with respect to the response obtained neglecting the motion-induced forces, is evaluated with reference to a square tall building with aspect ratio of 8. Results showed that the AMF does not exceed unity for reduced wind velocities lower than 10. Kawai (1992) carried out many wind tunnel tests on aeroelastic models corresponding to tall buildings with aspect ratio equal to 10 and different rectangular cross-sections. His results showed the influence of the turbulence intensity and the structural damping on the response for different cross-sections. Except for the side ratio $D/B = 0.5$, in general the vibrations reduce as the turbulence increases. Marukawa *et al.* in 1996 carried out wind tunnel aeroelastic tests using several stick models with different aspect and side ratios. The effects of the building shape and the structural damping on the aerodynamic damping ratios were derived. The results showed that in the acrosswind direction the aerodynamic damping ratio has first positive and increasing values and then becomes negative as the reduced velocity increases. The reduced velocity at which the aerodynamic damping becomes negative is influenced by the aspect ratio and the structural damping ratio. Gu and Quan (2004) assessed the influence of the aerodynamic damping on the acrosswind response of a square tall building with aspect ratio of 6 in different terrain exposures. The aerodynamic damping was found to become negative for reduced velocities greater than 10.

The across-wind response of tall buildings can be classified into three ranges of behaviour: the region where the aerodynamic damping is positive, the region where the vortex shedding produces the amplification of the response and the region where the structure experiences the galloping instability (Cheng *et al*. 2002). Although rare, it can also happen in slender structures that the critical galloping wind speed can be close to the vortex-resonance wind speed, thus provoking interactions between the two phenomena (Wawzonek and Parkinson 1979).

Beyond the empirical methods, approaches based on CFD are also currently used. They have the advantage of avoiding performing aeroelastic tests, but have the disadvantage of being very time consuming and sensitive to the correct choice of the parameters of the simulation (Braun and Awruch 2009).

The present paper proposes a semi-analytical method (Gabbai and Simiu 2010) based on wind tunnel tests carried out using rigid models and the analytical modeling of the wind forces. The procedure can be used to avoid performing aeroelastic tests on tall buildings. In the first part of the paper the possible onset of vortex excited oscillations or galloping instability for currently designed square tall buildings is discussed. It is pointed out that for the range of reduced velocities corresponding to the usual operational conditions of high-rise buildings, the acrosswind aeroelastic response lies in the regime of positive aerodynamic damping. Based on the aforementioned

estimation, a semi-analytical procedure is proposed to evaluate the aeroelastic response of square tall buildings accounting for the motion-induced forces in the range of positive aerodynamic damping. The procedure is theoretically applicable also to tall buildings with rectangular cross section but in this case, for wind blowing perpendicularly to the long side of the building, the reduced velocities for which the aerodynamic damping is positive is limited to smaller values (Kawai 1992, Marukawa *et al*. 1996). Therefore the range of applicability of the method for buildings with rectangular cross-sections is restricted to low reduced velocities.

The procedure requires as input the time histories of the local pressures measured in the wind tunnel on rigid models and proceeds through the direct integration of the equations of motion to compute the dynamic response of the structure accounting for motion-induced forces. The application of the semi-analytical procedure allows for the investigation of the applicability of wind tunnel data obtained from rigid models and demonstrates that for square tall buildings in operational conditions performing aeroelastic tests can be unnecessary, especially in the preliminary design phase. Moreover, in this method the actual modal shapes can be taken into account correctly in the evaluation of the structural response (Wu *et al*. 2008), instead of using simplified modal shapes as it is commonly done in aeroelastic models.

2. Across-wind aeroelastic response of square tall buildings

Literature references showing the results of aeroelastic tests on models of square tall buildings agree that in the acrosswind direction the structural response is amplified when a critical reduced velocity corresponding to the onset of vortex shedding resonance or galloping is exceeded, although the galloping of tall buildings has never been reported in literature.

The vortex shedding resonance occurs when the reduced velocity $U = V/fD$, where V is the top wind speed, f is the structural frequency in the acrosswind direction and D is the side length, is close to the critical value $U_{cr,v}$ corresponding to the reciprocal of the Strouhal number St

$$C_{cr,v} = \frac{1}{St} = \frac{V}{f_s D} \tag{1}$$

where f_s is the vortex shedding frequency. The Strouhal number for buildings with square cross-section is almost independent on the Reynolds number and is about 0.10 (Gu and Quan 2004, Hayashida and Iwasa 1990).

The critical velocity for galloping onset is influenced by many variables: the side length D, the damping ratio ξ, the natural frequency in the across-wind direction f and the mass density per unit height m. To evaluate the critical velocity of galloping, the Glauert-Den Hartog criterion can be applied, assuming that the quasi-steady theory is valid for every reduced velocity. According to the above mentioned criterion, the critical velocity for galloping is expressed by

$$V_{cr,g} = \frac{8\pi m f \xi}{\rho D(\partial C_L/\partial \alpha|_0 + C_D|_0)} \tag{2}$$

where $\partial C_L/\partial \alpha|_0 + C_D|_0$ is the galloping instability factor (Kwok 1977).

Fig. 1 shows the ratio of the critical galloping velocity and the wind speed at the top of a square building as a function of the reduced velocity and the mass-damping coefficient defined as

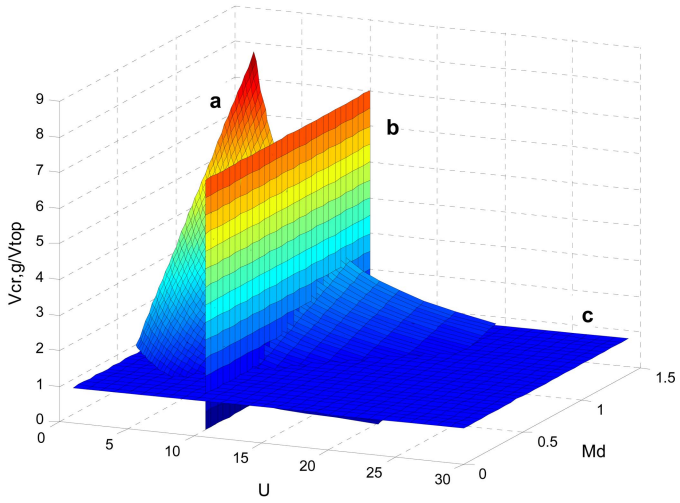

Fig. 1 Ratio of the critical galloping velocity and the wind speed at the top of the square building $V_{cr,g}/V_{top}$ as a function of the reduced velocity U and the mass damping coefficient M_d (a), plane $U_{cr,v}$=10 (b), plane $V_{cr,g}/V_{top}$=1 (c)

$$M_d = \frac{\int_0^H m(z)\Phi^2(z)dz}{\int_0^H \Phi^2(z)dz}\frac{\xi}{\rho D^2} \tag{3}$$

where m is the building's mass per unit height, Φ is the modal shape in the acrosswind direction and ρ is the air density. The critical reduced velocity of galloping, for any fixed value of the mass–damping coefficient, can be determined at the intersection between the surface and the plane $V_{cr,g}/V_{top} = 1$. Values of the ratio lower than unity correspond to the unsafe domain for galloping instability. The higher is the mass-damping coefficient, the higher is the critical reduced velocity for galloping $U_{cr,g}$, corresponding to the intersection between the surface and the plane $V_{cr,g}/V_{top} = 1$. If the galloping instability factor is assumed to be constant with the Reynolds number, the exposure conditions do not affect significantly the critical velocity for galloping. In the same Figure is shown the plane $U = 10$ that corresponds to the onset of vortex shedding resonance. As tall buildings are subjected to turbulent wind in which both the mean wind velocity and the turbulence intensity vary with height, a lock-in mechanism is activated and the excitation due to vortex shedding displays a broad band in the frequency domain. This modifies the structural response also at frequencies in the neighborhood of the frequency corresponding to the vortex resonance (Kwok and Melbourne 1981). For this reason most wind tunnel tests show that the across-wind aerodynamic damping begins to decrease for reduced velocities U lower than $U_{cr,v}$, typically beyond 8. Fig. 2 shows the across-wind aerodynamic damping ratio as a function of the reduced velocity for square tall buildings obtained from aeroelastic tests by Steckley (1989), Marukawa *et al.* (1996) and Gu and Quan (2004). The segment of positive aerodynamic damping is followed by a segment where the aerodynamic damping decreases until negative values are reached. In particular, the acrosswind aerodynamic damping has positive and increasing values for reduced velocities between 8 and 10. Beyond that range, the across-wind response of tall buildings is amplified due to lock-in excitation.

The critical reduced velocities for vortex shedding and galloping can be compared with those

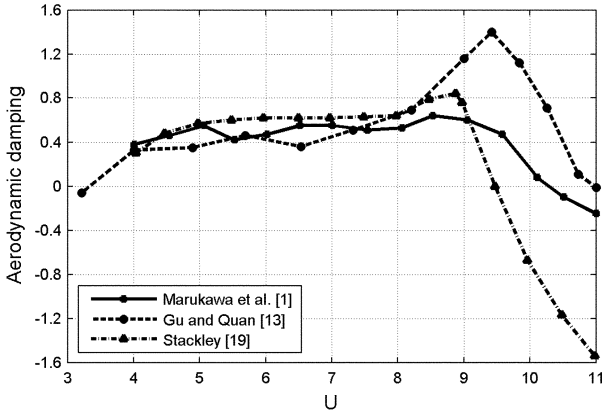

Fig. 2 Acrosswind aerodynamic damping ratio for square tall buildings

Table 1. Actual reduced velocities U for tall buildings in open terrain and urban terrain for V_{ref} = 30 m/s

Natural frequency (Hz)	Height (m)	Top mean wind speed in open terrain (m/s)	Reduced velocity in open terrain	Top mean wind speed in urban terrain (m/s)	Reduced velocity in urban terrain
0.10	500	56	14	71	18
0.15	333	53	9	65	11
0.2	250	50	6	61	8
0.25	200	48	5	58	6
0.3	167	47	4	56	5

Table 2. Mass-damping coefficients M_d for typical tall buildings

Damping ratio(%)	Mass density =130 kg/m^3	Mass density =180 kg/m^3	Mass density =230 kg/m^3
0.5	0.52	0.72	0.92
1.0	1.04	1.44	1.84
1.5	1.56	2.16	2.76
2.0	2.08	2.88	3.68

corresponding to ultimate limit state conditions for actual tall buildings. The reduced velocities for tall buildings in open terrain (α = 0.16, α is the exponent of the mean wind profile power law) and suburban terrain (α = 0.22) are reported in Table 1. They correspond to a reference wind speed of 30 m/s (10-minutes gust) that is a conservative value for non hurricane-prone regions. The natural frequency f varies between 0.10 and 0.30 Hz, where the lower bound is due to serviceability requirements and the upper bound due to the increased cost of more stiff buildings. As a first approximation the building's height can be computed using the simplified relationship H = 50/f .

Table 1 shows that the critical reduced wind speed corresponding to the beginning of the lock-in mechanism $U_{cr,v} \geq 8$ is not exceeded for buildings shorter than about 250 m. Such buildings comply with the design limitations on flexibility needed to warrant serviceability.

Table 2 shows the mass-damping coefficients M_d for actual tall buildings. The structural damping

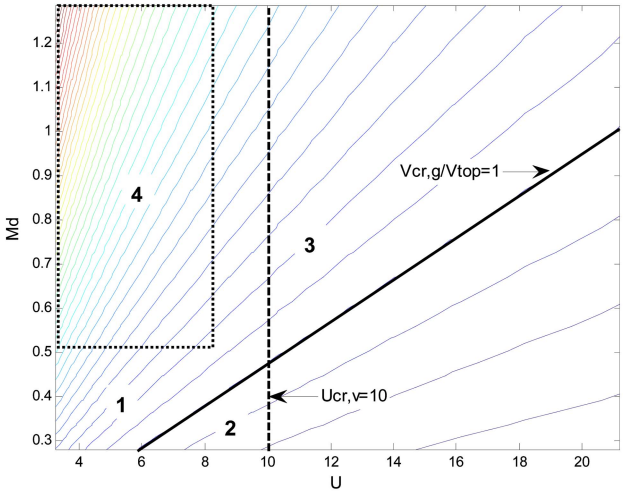

Fig. 3 Contour plot of the ratio between the critical galloping velocity and the wind speed at the top of the square building $V_{cr,g}/V_{top}$ as a function of the reduced velocity U and the mass-damping coefficient M_d

ratio ξ varies from 0.5 to 2.0 % of the critical value (Suda *et al*. 1996) and the mass density varies between 130 and 230 kg/m^3 (Boggs 1992).

Fig. 3 shows the contour plot of the ratio between the critical galloping velocity and the top wind speed as a function of the reduced velocity and the mass-damping coefficient. The line corresponding to the critical reduced velocity for vortex shedding resonance for square tall buildings ($U_{cr,v} = 10$) and the line corresponding to $V_{cr,g}/V_{top}$=1 are also shown. The lines divide the graph in several regions. Region 1 corresponds to the safe domain for both vortex shedding and galloping, region 2 corresponds to the unsafe domain for galloping and region 3 to the unsafe domain for vortex shedding. The rectangle that identifies region 4 corresponds to the behavior of actual tall buildings (Table 1 and 2). It can be noted that region 4 is a subset of region 1, i.e., the amplification of the acrosswind response due to aeroelastic phenomena can be negligible for square tall buildings in operational conditions because the aerodynamic damping is positive (Fig. 2).

3. Semi-analytical modeling of the motion – induced structural response of tall buildings

In this section a semi-analytical procedure is proposed to compute the wind-induced response of high-rise buildings accounting for aeroelastic effects. As discussed in Section 2, the procedure is based on the assumption that for square tall buildings and for reduced velocities corresponding to operational conditions, the structure is sufficiently far from experiencing vortex shedding resonance or galloping.

The proposed procedure consists of two phases. First of all, simultaneous measurements of the pressure time histories are taken in the wind tunnel on a rigid model, in order to obtain the aerodynamic forces. Then, aeroelastic forces are analytically evaluated and the structural response is computed through direct integration of the equations of motion considering the contribution of both the aerodynamic and aeroelastic forces.

3.1 Modeling of the aeroelastic forces

The equation of motion of a flexible structure excited by turbulent wind is

$$\boldsymbol{M}\ddot{\boldsymbol{q}}(t) + \boldsymbol{C}\dot{\boldsymbol{q}}(t) + \boldsymbol{K}\boldsymbol{q}(t) = \boldsymbol{F}(t) = \boldsymbol{F}_w(t) + \boldsymbol{F}_a(t) \tag{4}$$

where $\boldsymbol{M}$, $\boldsymbol{C}$, $\boldsymbol{K}$ are the mass, structural damping and stiffness matrices of the building, $\boldsymbol{q}(t)$, $\dot{\boldsymbol{q}}(t), \ddot{\boldsymbol{q}}(t)$ are the vectors collecting the structural displacement, velocities and accelerations, $\boldsymbol{F}_w(t)$ is the vector of the aerodynamic forces and $\boldsymbol{F}_a(t)$ is the vector of the aeroelastic forces induced by the movement of the structure.

To evaluate the aeroelastic forces $\boldsymbol{F}_a(t)$, the building is idealized as a simplified dynamic system having 3DOF for each floor, i.e., the translations along the cross-section's principal directions and the rotation around the vertical axis. Although the procedure can be extended to the general case, in the following the direction of the mean wind velocity at height z, $\overline{V}(z)$, is considered coincident with one of the cross section's principal directions (e.g axis x).

As shown in Fig. 5, the relative wind velocity in direction γ is V_r. Neglecting the floors' rotations,

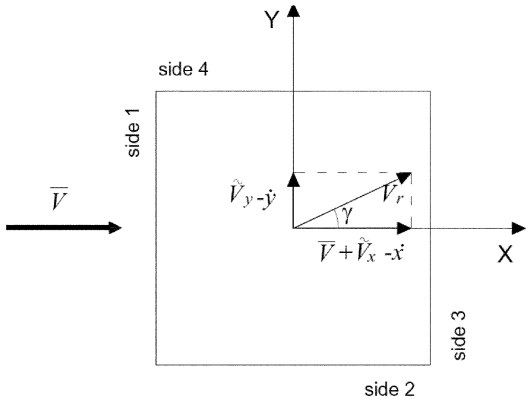

Fig. 4 Typical cross-section with axis orientation, sides numbering and wind speed components

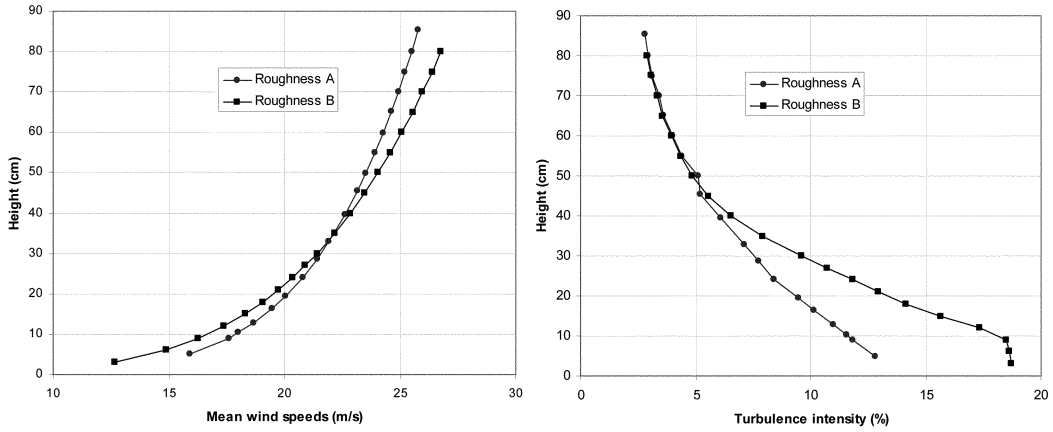

Fig. 5 Exponential approximation of the mean wind speed and turbulence intensity profiles for the two simulated terrain conditions

which are commonly small with respect to the angle γ, the alongwind component of the relative wind velocity at the height z is

$$V_{rx}(z,t) = \overline{V}(z) + \tilde{V}_x(z,t) - \dot{x}(z,t) \tag{5}$$

The acrosswind component of V_r at the height z is

$$V_{rx}(z,t) = \tilde{V}_y(z,t) - \dot{y}(z,t) \tag{6}$$

where $\overline{V}(z)$ is the mean wind speed of the undisturbed flow; $\tilde{V}_x(z,t)$, $\tilde{V}_y(z,t)$ are the turbulent components of the wind in the alongwind and acrosswind direction; $\dot{x}(z,t)$ and $\dot{y}(z,t)$ are the alongwind and acrosswind components of the structure's velocity at the elastic center.

The procedure takes advantage of the pressure coefficients measured in the wind tunnel on rigid models $C_{pi}(\gamma, z, t)$ for the relative wind velocity $V_r(z, t)$ forming an angle γ with the x axis. Each pressure coefficient is normalized with respect to the mean wind velocity at the height of each pressure tap. The resultant alongwind and acrosswind force coefficients can be computed, respectively, as follows

$$\begin{aligned} C_D(\gamma,z,t) &= \frac{1}{A(z)}\left[\sum_{i\in 1,3} C_{pi}(\gamma,z,t)A_i(z)\cos\gamma(t) + \sum_{i\in 2,4} C_{pi}(\gamma,z,t)A_i(z)\sin\gamma(t)\right] \\ C_L(\gamma,z,t) &= \frac{1}{A(z)}\left[\sum_{i\in 2,4} C_{pi}(\gamma,z,t)A_i(z)\cos\gamma(t) - \sum_{i\in 1,3} C_{pi}(\gamma,z,t)A_i(z)\sin\gamma(t)\right] \end{aligned} \tag{7}$$

where $A(z)$ is the total tributary area at height z and $A_i(z)$ is the tributary area of each pressure tap.

In the following, the dependency with the time is omitted for simplicity of notation.

The alongwind and acrosswind forces due to the relative wind speed $V_r(z)$ are

$$F_D(z) = \frac{1}{2}\rho A(z) C_D(\gamma,z) V_r^2(z) \tag{8}$$

$$F_L(z) = \frac{1}{2}\rho A(z) C_L(\gamma,z) V_r^2(z) \tag{9}$$

where ρ is the air density.

The projection of $F_D(z)$ and $F_L(z)$ along the x and y axes are

$$\boldsymbol{F}(z) = \begin{Bmatrix} F_x(z) \\ F_y(z) \end{Bmatrix} = \frac{1}{2}\rho A V_r^2(z) \begin{Bmatrix} C_D(\gamma)\cos\gamma - C_L(\gamma)\sin\gamma \\ C_L(\gamma)\sin\gamma + C_D(\gamma)\cos\gamma \end{Bmatrix} \tag{10}$$

By substituting the expressions $\sin\gamma = \dfrac{\tilde{V}_y - \dot{y}}{|V_r|}$ and $\cos\gamma = \dfrac{\overline{V} + \tilde{V}_x - \dot{x}}{|V_r|}$, Eq. (10) becomes

$$\boldsymbol{F}(z) = \frac{1}{2}\rho A V_r(z) \begin{Bmatrix} C_D(\gamma)(\overline{V} + \tilde{V}_x - \dot{x}) - C_L(\gamma)(\tilde{V}_y - \dot{y}) \\ C_D(\gamma)(\tilde{V}_y - \dot{y}) + C_L(\gamma)(\overline{V} + \tilde{V}_x - \dot{x}) \end{Bmatrix} \tag{11}$$

Adopting the following approximations

$$\begin{aligned} V_r(\overline{V}+\tilde{V}_x-\dot{x}) &= \overline{V}^2+2\overline{V}\tilde{V}_x-2\overline{V}\dot{x} \\ V_r(\tilde{V}_y-\dot{y}) &= \overline{V}\tilde{V}_y-\overline{V}\dot{y} \end{aligned} \tag{12}$$

Eq. (11) becomes

$$\boldsymbol{F}_a(z) = \frac{1}{2}\rho A\begin{cases} C_D(\gamma)(\overline{V}^2+2\overline{V}\tilde{V}_x-2\overline{V}\dot{x})-C_L(\gamma)(\overline{V}\tilde{V}_y-\overline{V}\dot{y}) \\ C_D(\gamma)(\overline{V}\tilde{V}_y-\overline{V}\dot{y})+C_L(\gamma)(\overline{V}^2+2\overline{V}\tilde{V}_x-2\overline{V}\dot{x}) \end{cases} \tag{13}$$

The force $\boldsymbol{F}(z)$ can be written as the difference between the aerodynamic force $\boldsymbol{F}_w(z)$ and the aeroelastic force $\boldsymbol{F}_a(z)$. While the aerodynamic forces are directly available from the pressure coefficient time histories measured in the wind tunnel, the aeroelastic forces are calculated as

$$\boldsymbol{F}_a(z) = -\rho A\overline{V}\begin{cases} C_D(\gamma)\dot{x}-\dfrac{1}{2}C_L(\gamma)\dot{y} \\ \dfrac{1}{2}C_D(\gamma)\dot{y}+C_L(\gamma)\dot{x} \end{cases} \tag{14}$$

In terms of pressure coefficients, Eq. (14) becomes

$$\boldsymbol{F}_a(z) = -\rho\overline{V}\begin{cases} \left[\sum_{i\in 1,3} C_{pi}(\gamma,z,t)A_i(z)\cos\gamma+\sum_{i\in 2,4} C_{pi}(\gamma,z,t)A_i(z)\sin\gamma\right]\dot{x}+ \\ -\frac{1}{2}\left[\sum_{i\in 2,4} C_{pi}(\gamma,z,t)A_i(z)\cos\gamma+\sum_{i\in 1,3} C_{pi}(\gamma,z,t)A_i(z)\sin\gamma\right]\dot{y} \\ \frac{1}{2}\left[\sum_{i\in 1,3} C_{pi}(\gamma,z,t)A_i(z)\cos\gamma+\sum_{i\in 2,4} C_{pi}(\gamma,z,t)A_i(z)\sin\gamma\right]\dot{y}+ \\ +\left[\sum_{i\in 2,4} C_{pi}(\gamma,z,t)A_i(z)\cos\gamma+\sum_{i\in 1,3} C_{pi}(\gamma,z,t)A_i(z)\sin\gamma\right]\dot{x} \end{cases} \tag{15}$$

The aeroelastic forces in Eq. (15) can be incorporated in the structural analysis by adding the aerodynamic damping matrix $\boldsymbol{C_a}$ to the structural damping matrix $\boldsymbol{C}$. Therefore Eq. (4) becomes

$$\boldsymbol{M}\ddot{\boldsymbol{q}}(t)+(\boldsymbol{C}+\boldsymbol{C_a})\dot{\boldsymbol{q}}(t)+\boldsymbol{K}\boldsymbol{q}(t) = \boldsymbol{F_w}(t) \tag{16}$$

In Eq. (16), $\boldsymbol{C_a}$ is the aerodynamic damping matrix which stores on the principal diagonal the matrices $C_{a,k}$ of the aerodynamic damping of the floors of the building

$$\boldsymbol{C_a} = \begin{bmatrix} \ldots & 0 & 0 & \ldots \\ 0 & C_{a,k} & 0 & 0 \\ 0 & 0 & C_{a,k+1} & 0 \\ \ldots & 0 & 0 & \ldots \end{bmatrix} \tag{17}$$

The generic aerodynamic damping matrix of the k-th floor of the building has the form

$$\boldsymbol{C}_{a,k} = \rho\overline{V}\begin{bmatrix} \left[\sum_{i\in 1,3} C_{pi}(\gamma,z,t)A_i(z)cos\gamma + \sum_{i\in 2,4} C_{pi}(\gamma,z,t)A_i(z)sin\gamma\right] & -\frac{1}{2}\left[\sum_{i\in 2,4} C_{pi}(\gamma,z,t)A_i(z)cos\gamma - \sum_{i\in 1,3} C_{pi}(\gamma,z,t)A_i(z)sin\gamma\right] & 0 \\ \left[\sum_{i\in 2,4} C_{pi}(\gamma,z,t)A_i(z)cos\gamma - \sum_{i\in 1,3} C_{pi}(\gamma,z,t)A_i(z)sin\gamma\right] & \frac{1}{2}\left[\sum_{i\in 1,3} C_{pi}(\gamma,z,t)A_i(z)cos\gamma - \sum_{i\in 2,4} C_{pi}(\gamma,z,t)A_i(z)sin\gamma\right] & 0 \\ 0 & 0 & 0 \end{bmatrix} \tag{18}$$

In Eq. (18), the pressure coefficients at time t correspond to the direction of instantaneous attack γ. As γ varies with time, the set of pressure coefficients which are used for the computation of the aerodynamic damping matrix varies. If a limited number of sets of pressure coefficients corresponding to a limited number of attack angles are available from wind tunnel tests, a linear interpolation among the available sets of measurements can be performed.

4. Application of the proposed procedure

The proposed procedure was applied to a square tall building 240 m high and 40 m wide, with an aspect ratio of 6. Wind tunnel tests were carried out on a rigid model of the building instrumented with pressure taps to obtain the pressure coefficient time histories for two different terrain exposures. Then, data was used to evaluate the structural response accounting for aerodynamic damping. Finally, results were validated with results found in the literature, obtained by aeroelastic tests.

4.1 Wind tunnel tests

Experimental tests were carried out in the boundary-layer wind tunnel operated by CRIACIV (Inter-university Research Center on Buildings Aerodynamic and Wind Engineering) in Prato, Italy. It is an open circuit tunnel with dimensions of the working section B_w = 2.4 m, H_w = 1.6 m.

The length scale of the model was 1/650. The model was equipped with 120 pressure taps, 30 for each side. Tests were carried out with wind speed profiles and turbulence intensity corresponding to open terrain (roughness A) and suburban terrain conditions (roughness B). The exponents of the mean wind profiles were α = 0.17 and α = 0.22, respectively. Fig. 5 shows the mean wind speed and the longitudinal turbulence intensity profiles for the simulated terrain conditions.

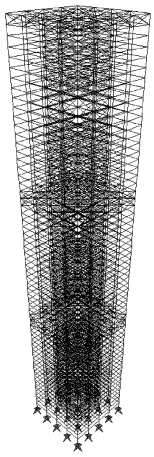

Fig. 6 3D view of the finite element model

4.2 Structural modeling

The structure is made of steel with central cores and systems of bracings in both the principal directions (Fig. 6). Floors are reinforced concrete slabs capable of rigid in-plane behaviour. The structure was modelled as a simplified dynamic system having 3DOF's for each floor obtained by static condensation from a finite element model of the structure. The stiffness matrix was computed by inverting the flexibility matrix assembled from the generalized displacements obtained by applying unit forces at the center of mass of each floor. The first three natural frequency of the building are 0.208 Hz, 0.215 Hz and 0.287 Hz.

4.3 Wind load modeling

The pressure coefficient time histories were obtained from the wind tunnel tests. The procedure was applied using both the roughness conditions used for the wind tunnel tests.

The reference velocity was varied in order to have the reduced wind speed at the top of the building ranging from 1 to 8. The latter value represents a conventional upper bound for the application of the procedure, one that gives a conservative estimate of the limit of positive aerodynamic damping.

To make the pressure time histories measured in the wind tunnel representative of the real phenomenon, the similitude criterion on the reduced frequency, as it is usually done for tall buildings, was applied

$$\frac{n_m \cdot D_m}{V_m} = \frac{n_p \cdot D_p}{V_p} \tag{19}$$

where $n = 1/\delta t$ is the frequency of the forcing function, V is the mean wind speed at height H and D is the side length. The subscript m refers to the model while the subscript p to the prototype.

The time interval $\delta t = 1/n_p$ used for the integration of the equations of motion is therefore

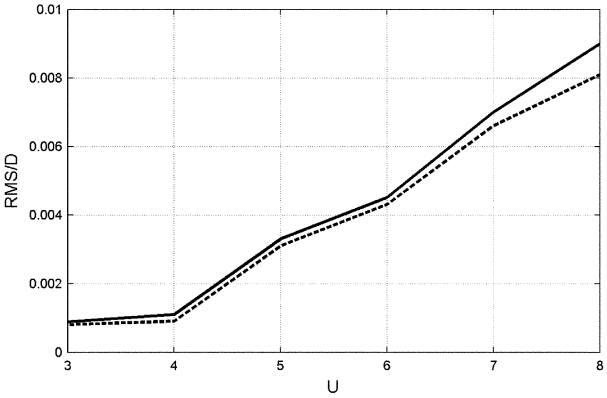

Fig. 7 Normalized RMS top acrosswind displacements obtained with (solid line) and without (dashed line) the contribution of the aeroelastic forces in open terrain

$$\delta t = \frac{D_p \cdot V_m}{D_m \cdot V_p \cdot n_m} \tag{20}$$

4.4 Results and validation

The proposed procedure was applied to the case study to assess the structural response taking into account the wind-structure interaction.

In Fig. 7 the RMS acrosswind displacements at the top of the building obtained with and without the contribution of the aeroelastic forces in open terrain are compared. In both cases the acrosswind response increases with the reduced velocity as well as the difference between the responses. This behaviour confirms the growth of the aerodynamic damping with the reduced velocity.

To have a proper indicator of the importance of the aeroelastic response, the equivalent aerodynamic damping ratio is evaluated. It is the value ξ_{eq} that minimizes the function $f(\xi)$, where $f(\xi)$ is the relative difference between the maximum displacement at the top of the building obtained with a trial equivalent damping ratio $x_{\max}(\xi)$ and with the motion-induced forces $x_{a,\max}$. The function is minimized using a Newton-Raphson procedure until

$$f(\xi_i) = \frac{x_{\max}(\xi_i) - x_{a,\max}}{x_{a,\max}} < \delta \tag{21}$$

where the tolerance δ for the convergence problem is 10^{-3}.

To statistically characterize the equivalent aerodynamic damping ratio, the response time histories were divided into a large number of intervals, each one 600 s long, allowing windows to overlap. Then, the mean value of the equivalent aerodynamic damping ratios was computed. Fig. 8 shows the acrosswind equivalent aerodynamic damping ratio computed using the proposed procedure, as a function of the reduced velocity for open and suburban terrain conditions. The equivalent aerodynamic damping increases with the reduced velocity and for higher turbulence intensity the aerodynamic damping is smaller, in agreement with literature results (Gu and Quan 2004). In the same figure, the results are compared to those by Marukawa *et al*. (1996), Stackley (1989), Quan *et al*. (2005) obtained in slightly different testing conditions.

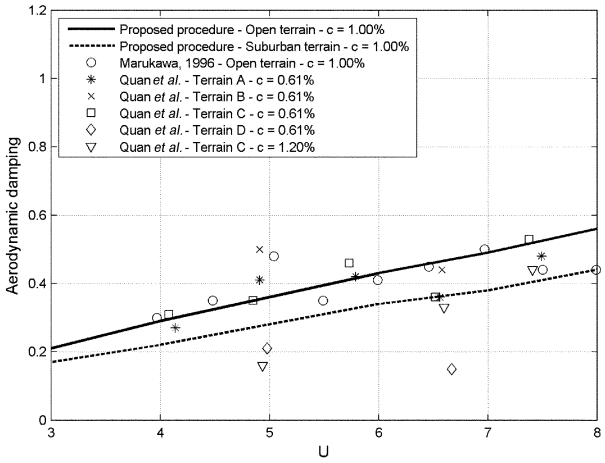

Fig. 8 Acrosswind aerodynamic damping ratio

The results obtained with the semi-analytical model are in agreement with the empirical results found in the literature. Results demonstrate that the acrosswind response of the buildings is properly evaluated using data from wind tunnel tests on a rigid model and considering the numerically computed aerodynamic damping.

5. Conclusions

The present paper is aimed at investigating the possibility of using wind tunnel data obtained from rigid models for the design of square tall buildings. For this purpose, a semi-analytical procedure for the evaluation of the aeroelastic response of square tall buildings is proposed.

The aerodynamic forces are measured in the wind tunnel on rigid models, while the contribution of the aeroelastic forces is taken into account through a time-dependent aerodynamic damping matrix evaluated using the pressure field around the building. The correspondent equivalent aerodynamic damping ratio can be computed using a Newton-Raphson procedure and the structural response can be evaluated through direct integration of the equations of motion.

The procedure proved to be successfully applicable in the range of positive aerodynamic damping that corresponds to the operational reduced velocities of most tall building lower than about 250 m. In that range, the aerodynamic damping computed using the proposed procedure seems to correctly represent the one evaluated using wind tunnel tests on flexible models reported in the literature. Thus, in the range of positive aerodynamic damping, the proposed procedure can be used as a substitution of expensive testing on flexible models.

References

Amandolese, X. and Hemon, P. (2010), "Vortex-induced vibration of a square cylinder in wind tunnel", C. *R. Mecanique*, **338**(1), 12-17.

Boggs, D.W. (1992), "Validation of the aerodynamic model method", *J. Wind Eng. Ind. Aerod.*, **42**(1-3), 1011-

1022.
Braun, A.L. and Awruch, A.M. (2009), "Aerodynamic and aeroelastic analyses on the CAARC standard tall building model using numerical simulation", *Comput Struct*., **87**(9-10), 564-581
Cheng, C.M., Lu, P.C. and Tsai, M.S. (2002), "Acrosswind aerodynamic damping of isolated square-shaped buildings", *J. Wind Eng. Ind. Aerod*., **90**(12-15), 1743-1756.
Gabbai, R.D. and Simiu, E. (2010), "Aerodynamic damping in the along-wind response of tall buildings", *J. Struct. Eng.- ASCE*, **136**(1), 117-119.
Gu, M. and Quan, Y. (2004), "Across-wind loads of typical tall buildings", *J. Wind Eng. Ind. Aerod*., **92**(13), 1147-1165.
Hayashida, H. and Iwasa, Y. (1990), "Aerodynamic shape effects for tall building for vortex induced vibration", *J. Wind Eng. Ind. Aerod*., **33**(1-2), 237-242.
Kawai, H. (1992), "Vortex induced vibration of tall buildings", *J. Wind Eng. Ind. Aerod*., **41**(1-3), 117-128.
Kawai, H. (1998), "Effect of corner modifications on aeroelastic instabilities of tall buildings", *J. Wind Eng. Ind. Aerod*., **74-76**, 719-729.
Kim, Y. and Kanda, J. (2010) "Effects of taper and set back on wind force and wind-induced response of tall buildings", *Wind Struct*., **13**(6), 499-517.
Kwok, K.C.S. and Melbourne, W.H. (1981), "Wind induced lock-in excitation of tall structures", *J. Struct. Div.- ASCE*, **107**(1), 57-72.
Kwok, K.C.S. (1977), *Cross-wind response of structures due to displacement dependent excitations*, Ph.D. Thesis, Monash University, Victoria, Australia.
Marukawa, H., Kato, N., Fujii, K. and Tamura, Y. (1996), "Experimental evaluation of aerodynamic damping of tall buildings", *J. Wind Eng. Ind. Aerod*., **59**(2-3), 177-190.
Novak, M. (1972), "Galloping oscillations of prismatic structures", *J. Eng. Mech. Div*., **98**(EM1), 27-46.
Quan, Y., Gu, M. and Tamura, Y. (2005), "Experimental evaluation of aerodynamic damping of square super high-rise buildings", *Wind Struct*., **8**(5), 309-324.
Stackley, A. (1989), *Motion-induced wind forces on chimneys and tall buildings*, PhD Thesis, University of Western Ontario.
Suda, K., Satake, N., Ono, J. and Sasaki, A. (1996), "Damping properties of buildings in Japan", *J. Wind Eng. Ind. Aerod*., **59(2-3)**, 383-392.
Vickery, B.J. and Steckley, A. (1993), "Aerodynamic damping and vortex excitation on an oscillating prism in turbulent shear flow", *J. Wind Eng. Ind. Aerod*., **49**, 121-140.
Washizu, K., Ohya, A., Otsuki, Y. and Fujii, K. (1978), "Aeroelastic instability of rectangular cylinders in a heaving mode", *J. Sound Vib*., **59**(2), 195-210.
Wawzonek, M.A. and Parkinson, G.V. (1979), "Combined effects of galloping instability and vortex resonance, *Proceedings of the 5th Int. Conf. Wind Engineering*, Fort Collins, 673-684.
Wu, H.Y., Liang, S.G., Chen, Z.Q. and Peng, X.H. (2010) "Research on the aerodynamic damping ratios of square tall buildings in across-wind direction under strong wind", *Gongcheng Lixue/Eng. Mech*., **27**(10), 96-103.
Wu, J.R., Li, Q.S. and Tuan, A.Y. (2008) "Wind induced lateral-torsional response of tall buildings", *Wind Struct*., **11**(2), 153-178.

CC